Applied Radiation and Isotopes 130 (2017) 153–161

Contents lists available at ScienceDirect

Applied Radiation and Isotopes

journal homepage: www.elsevier.com/locate/apradiso

Determination of trace elements in calcium rich carbonate rocks by Wavelength Dispersive X-ray Fluorescence Spectrometry for environmental and geological studies

T.Yu. Cherkashina*, S.I. Shtel'makh, G.V. Pashkova

Institute of the Earth's Crust, SB RAS, 128 Lermontov St., Irkutsk 664033, Russia

HIGHLIGHTS

- The WDXRF technique was developed for the sedimentary rocks with high Ca content.
- Infinitely thick samples were prepared.
- The calibration data were obtained using the sediment and rock reference materials.
- V, Cr, Co, Ni, Cu, Zn, Pb, Ba, La, Ce, Nd, Rb, Sr, Y, Zr, Nb were determined.
- Analytical figures of merit were found to be satisfactory.

ARTICLE INFO

Keywords:
Calcium rich carbonate
Marble
Fluorite ore
Carbonatite-like rocks
WDXRFS
Analytical figures of merit

ABSTRACT

A simple, rapid and non destructive Wavelength Dispersive X-ray Fluorescence Spectrometry (WDXRFS) was developed for the determination of trace elements such as V, Cr, Co, Ni, Cu, Zn, Pb, Ba, La, Ce, Nd, Rb, Sr, Y, Zr, and Nb in carbonate rocks with high calcium content. Samples of marble, limestone, fluorite ore and carbonatite-like rocks were chosen as objects under investigation. These samples have wide ranges of major and trace element contents, and high concentration of calcite (70–98%) in calcium rich carbonates. The sample mass required for infinite thickness was calculated for each element. In order to determine V, Cr, Co, Ni, Cu, Zn, Ba, La, Nd, Ce, sample weighting 1 g was pressed with a pressure of 100 kN. For the determination of Rb, Sr, Y, Zr, Nb, Pb, the sample mass was increased up to 5 g. The calibration curves were constructed by employing the International Certified reference materials (ICRMs) and in-house standard reference materials (HSRMs) of various types of rocks and sediments, and the matrix effects were taken into account using the influence coefficients (α-correction equations). Analytical figures of merit have also been assessed. The calculated values of the instrumental limit of the detection were within the interval from 0.5 to 4.0 mg kg^{-1}. The repeatability and reproducibility were found to be satisfactory with the relative standard deviations lower than 5%. The accuracy was evaluated by the analysis of two reference materials and the comparison with the ICP-MS results. A good agreement was achieved between the reference and measured values with recoveries ranging from 85% to 115%. The relative disagreements between the XRF and ICP-MS results were less than 10%.

1. Introduction

A comprehensive study of geological and geochemical characteristics of carbonate sedimentary rocks usually involves the determination of chemical composition of samples studied. Obtained geochemical data about spatial distribution of different elements can be used for determining the origin of the carbonate rocks, understanding the nature of modern carbonates, interpreting processes and products of diagenesis, etc. (James and Jones, 2015; Letnikova, 2005; Sklyarov et al., 2001). In geologic study carbonatite and carbonatite-like rocks, the major and trace elements can serve as an indicators of Late Riphean rifting, which took place in the Siberian craton (Savel'eva et al., 2014). Geoecologycal and geochemical investigations of sediments and sedimentary rocks are performed in (Santos et al., 2007; Zwolinski et al., 2007; Markov, 2011) to reconstruct paleogeochemical conditions of the sedimentation and to identify the main factors controlling their accumulation.

In the present research, studied samples of the sedimentary rocks

* Corresponding author.
E-mail address: tcherk@crust.irk.ru (T.Y. Cherkashina).

http://dx.doi.org/10.1016/j.apradiso.2017.09.038
Received 26 August 2016; Received in revised form 19 July 2017; Accepted 22 September 2017
Available online 23 September 2017

were collected from two areas: central part of the Republic of Buryatia and western shore of Lake Baikal (Russia). These samples have wide ranges of major and trace element contents, and high concentration of calcite: in carbonate samples the calcite content is from 90% to 98%, in carbonatite samples – 70–90%. Concentrations of the major oxides in various types of the carbonates, for instance, dolomite (Wheeler, 1999), limestone (Wheeler, 1999; Arriolabengoa et al., 2015; Babatunde and Ademola, 2014), magnesite (Jones and Wilson, 1991), and marl (Arriolabengoa et al., 2015), can be successfully determined using X-ray fluorescence (XRF) method. However, in geochemical and ecological studies the bulk chemical composition of the carbonate rocks is not fairly informative without experimental data about the accumulation and spatial distribution of the trace elements (Letnikova, 2005; Sklyarov et al., 2001). As is known, carbonate materials is characterized by low concentration levels of most of the trace elements (Revenko, 2002). In fact, usage of the WDXRF method can be limited due to the poor sensitivity for some elements. Moreover, there is a general lack of the International Certified reference materials (ICRMs) and the in-house standard reference materials (HSRMs) of the carbonate rocks suitable for analyzing the diversity of the trace elements (Revenko, 2002; Sliwinski et al., 2012; Sarbajna et al., 2013).

Main objective of our research is to develop WD X-ray fluorescence (WDXRF) technique, in particular, generate the best analytical strategy for the determination of the selected trace elements to study the genesis of the sedimentary carbonates and carbonatites. Within the investigation, we consider the following steps: (i) choice and performing the sample preparation procedure; (ii) analyzing carbonate, carbonatite (veined carbonated and carbonatic-siliziclastic rocks), and fluorite ore samples by the XRF spectrometry including the choice of optimal conditions of the measurement; (iii) computing concentrations of some trace elements (V, Cr, Co, Ni, Cu, Zn, Pb, Ba, La, Ce, Nd, Rb, Sr, Y, Zr, and Nb), which are indicators of the paleogeochemical conditions of the sedimentation; (iv) performing the correction of the matrix effects; (v) validating analytical figures of merit for the developed XRF technique.

2. Methodology

2.1. Sample collection and processing

All studied samples were collected from two areas: central part of the Republic of Buryatia and western shore of Lake Baikal. Geographical setting of these areas is the following.

Zaigraevskii area is located in central part of the Buryatia Republic (109°15′N and 52°50′E). Area of the Zaigraevskii district is equal to 6603 km^2. It bounders with the Baikal region (Ulan-Ude town) in the north and Zabaikal'skii area in the south (Zaigraevskii area, 2015). Biliutinsky deposit is a part of the Zaigraevskii district and located 80 km north of the Ulan-Ude town. Nowadays, chemically pure limestones of the Biliutinsky deposit are used for the production of different types of chemical materials such as carbide of calcium and silicon, acetylene, lime chloride, and others. Also these limestones are applied in metallurgy, paper-pulp and building industry (Mineral resources of the Republic of Buryatia, 2015). The representative limestone, marble, carbonate and fluorite ore samples were collected by S.I. Shtel'makh from a bottom part of dikes of granite-porphyry, andesite, trachyte composition of the Biliutinsky deposit.

The carbonatite-like rocks are appearing along the western shore of the Lake Baikal, a south part of the Siberian craton. The carbonatite rocks occur in the form of veins a few centimeters thick and fragments up to 10 cm among gneisses and granites. The rocks are yellow-gray or brown-colored and consist of carbonate 70–90% (Savel'eva et al., 2014). The carbonatite-like samples weighing about 15 kg were collected from calcitic and dolomitic veins at three sampling sites located approximately 10 km away from each other.

The cone and quartering sample preparation was applied for the obtaining a representative sample. The sample preparation has been performed with requirements given in (OST, 2004). The collected samples were manually grinded and homogeneously mixed in an agate mortar for 10 h. For the elimination of a particle aggregation during the milling process a few drops of an ethyl hydroxide of high purity were added. Particle sizes of the powdered samples were defined using a laser particle-size analyzer “Analysette 22” COMPACT (FRITSCH, Germany). The determined sizes of the particles are in the range from 10 to 61 μm. Then the weighing procedure was conducted as follows. For the determination of Rb, Sr, Y, Zr, Nb, Pb each sample powder weighing 5 ± 0.001 g and wax weighing 1 ± 0.001 g as a binding agent was taken using an analytic balance of AB-series (St. Petersburg, Russia). Then these components were mixed and thoroughly shaken for two minutes. For the determination of the V, Cr, Co, Ni, Cu, Zn, Ba, La, Ce, Nd contents, each sample powder weighing 1 ± 0.001 g was also taken using the analytic balance. Prepared samples were pressed on the basis with boric acid using a HERZOG HTP-40 semiautomatic press with a pressure of 100 kN.

2.2. WDXRF set-up

All measurements were carried out in a vacuum condition using a WDXRF spectrometer S8 TIGER (Bruker AXS, Germany). This instrument is equipped with a 4 kW power X-ray tube with a rhodium anode and a beryllium window of 75 μm thickness. Detailed information about the WDXRF-spectrometer features can be found elsewhere (Service Manual, 2007). Listed in Table 1 are the instrumental measuring conditions used.

To select the optimal crystal, we measured the intensities of peaks and backgrounds for the analytical CrK$_\alpha$-, LaL $_\alpha$-, and Sr K$_\alpha$- lines using LiF(200) and LiF(220) crystals and a 0.23° collimator. The comparison of the intensity levels of the peaks and backgrounds for these elements and the calculated WDXRF spectrum contrast (peak-to-background ratio) values of their spectra for the LiF(200) and LiF(220) crystals was carried out (Table 2, Figs. 1–3). It can be seen, that for our WDXRF spectrometer, S8 TIGER, with a comparable contrast on the LiF(200) and LiF(220) crystals, measurements on the LiF(200) crystal provide higher count rate by 1.3–2 times. In our opinion, this is due to the fact that in this wavelength region the scattered bremsstrahlung of the X-ray tube is not the dominant background component for our spectrometer. For all measurements, the authors applied an universally usable crystal of LiF(200) which has higher reflectivity, rather than LiF(220), and can used for the elements with atomic number 19 (K) onwards (Schlotz, 2006). LiF(220) has lower reflectivity but higher resolution than LiF (200) (Schlotz, 2006). Thus, our choice of the LiF(200) crystal for determining the V, Cr, Co, Ni, Cu, Zn, Pb, Ba, La, Ce, Nd, Rb, Sr, Y, Zr, and Nb contents was responsible for the above arguments and the obtained experimental data.

Measurement time of the analytical line and the background from each element was 60–100 s and 30–60 s, respectively. Processing the X-ray spectra, numerical peak separation, and the correction of the matrix effects were performed using the software SPECTRA^{plus} (SPECTRA 2010) linked to the equipment.

2.3. Reference materials

The analytical quality control and construct of calibration curves were carried out using the ICRMs and HSRMs of different types of rocks and sediments with high content of calcium (more than 25%): carbonatite Bronnitsky (4390-88), fluorite FM (2979-81), GPOS301 and GPOS302 (dolo limestones), GPOS303 (feldspar dolo limestone), OOPE401 (calcareous ooze) (Arnautov, 1990; Govindaraju, 1994).

The available ICRMs and HSRMs only partially cover possible variations of the concentrations of the elements determined. The possibility of the usage of the ICRMs and HSRMs of the different composition rocks in a single calibration set was showed in (Revenko, 2002) to provide wide range of the element contents determined. Thus, the rock

Table 1
WDXRF measuring conditions.

Analytical line	2θ (°)		kV	mA	Filter, thickness (μm)	Collimator (°)	Detector
	Peak	Back-ground					
$VK_{\alpha1}$	76.92	75.63	50	40	Al, 12.5	0.17	FPC[a]
$CrK_{\alpha1}$	69.39	68.49	50	40	Al, 200	0.23	SC[b]
$CoK_{\alpha1}$	52.79	53.81	50	50	Al, 200	0.17	SC
$NiK_{\alpha1}$	48.68	48.00	50	50	Al, 100	0.23	SC
$CuK_{\alpha1}$	45.04	45.54	50	50	Al, 200	0.17	SC
$ZnK_{\alpha1}$	41.81	41.08	50	50	Al, 500	0.17	SC
$PbL_{\beta1}$	28.25	28.73	50	50	Al, 500	0.17	SC
$RbK_{\alpha1}$	26.61	25.80	50	40	Al, 500	0.17	SC
$SrK_{\alpha1}$	25.14	25.80	50	50	Al, 500	0.17	SC
$YK_{\alpha1}$	23.70	24.29	50	40	Al, 500	0.17	SC
$ZrK_{\alpha1}$	22.50	21.02	50	40	Al, 500	0.17	SC
$NbK_{\alpha1}$	21.39	21.02	50	40	Al, 500	0.17	SC
$BaL_{\alpha1}$	87.17	87.90	50	40	None	0.17	FPC
$LaL_{\alpha1}$	82.95	82.40	50	40	None	0.23	FPC
$CeL_{\beta1}$	71.64	71.00 72.93	50	40	None	0.17	SC
$NdL_{\alpha1}$	72.16	71.00 72.93	50	40	None	0.17	SC

[a] Flow Proportional Counter.
[b] Scintillator Counter.

Table 2
WDXRF spectrum contrast for the CrK_{α}-, SrK_{α}- and LaL_{α}-lines.

Line	Crystal	Peak intensity, KCps	Background intensity, KCps	WDXRF spectrum contrast
CrK_{α}	LiF200	0.390	0.076	5
CrK_{α}	LiF220	0.174	0.040	4.4
SrK_{α}	LiF200	30.99	1.60	19
SrK_{α}	LiF220	19.13	1.10	19
LaL_{α}	LiF200	9.17	0.30	30
LaL_{α}	LiF220	7.32	0.25	29

WDXRF spectrum contrast was calculated for the RMs with the following contents: Cr (260 mg kg^{-1}), Sr (1200 mg kg^{-1}) and La (19,300 mg kg^{-1}).

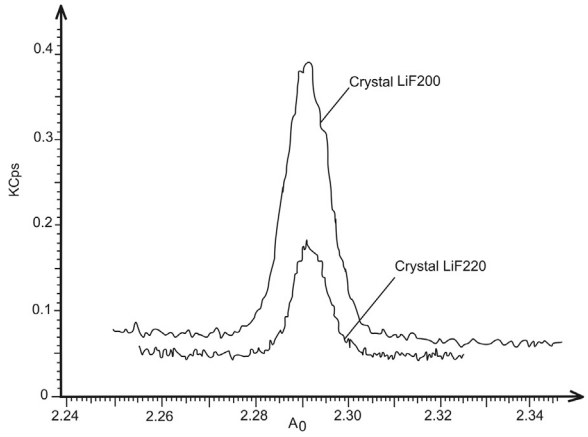

Fig. 1. XRF spectrum of the CrK_{α}-line (measurement time is 1200 s).

the ICRMs and HSRMs of various chemical compositions were added to the calibration set. These rock reference materials are OOKO202 (background sediment), OOKO204 (anomalous sediment), OOKO302 (anomalous silt), OOKO303 (background silt), OOPE101 (terrigenous clay), OOPE201 (terrigenous silt), OOPE402 (siliceous silt), DVG (greisenized granite), DVB (bipyroxene basaltic andesite), DVD (hornblende dacite), DVM (olivine-rich meymechite), MO3 (gabbro) (Arnautov, 1990; Govindaraju, 1994). These HSRMs were produced by Czechoslovak Socialist Republic, Bronnitskaya geological-geochemical expedition at the Federal State Unitary Enterprise "Institute of

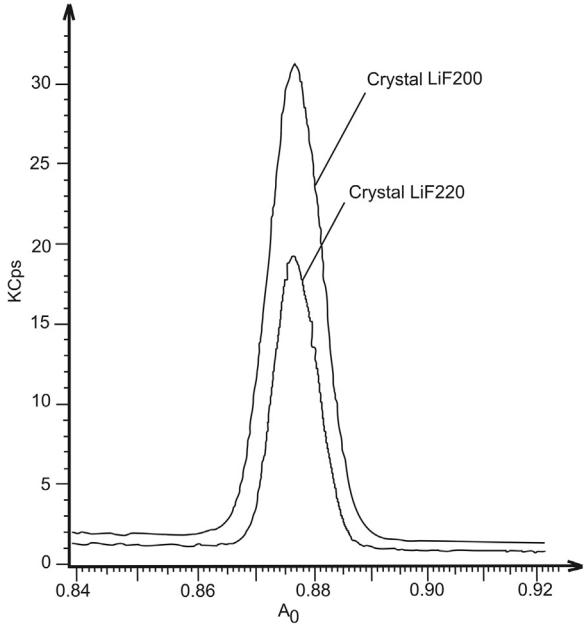

Fig. 2. XRF spectrum of the SrK_{α}-line (measurement time is 600 s).

Mineralogy, Geochemistry and Crystal Chemistry of Rare Elements" in Russia (Bronnitskaya expedition, 1970), the Institute of Geochemistry, Siberian Branch of Russian Academy of Sciences in Russia (Catalog of Reference Materials, 2013), the Applied Physics Institute at Irkutsk State University in Russia (API ISU, 1970).

3. Result and discussions

3.1. Characterization of marble, limestone, fluorite ore and rocks like carbonatites

The light-gray limestone, light- and dark- gray, and white marble, fluorite ore carbonatite-like rock samples were selected as objects of the research. All collected samples have different mineral constituents and wide variations of their chemical composition. The mineral composition of these samples was determined by X-ray diffraction analysis using

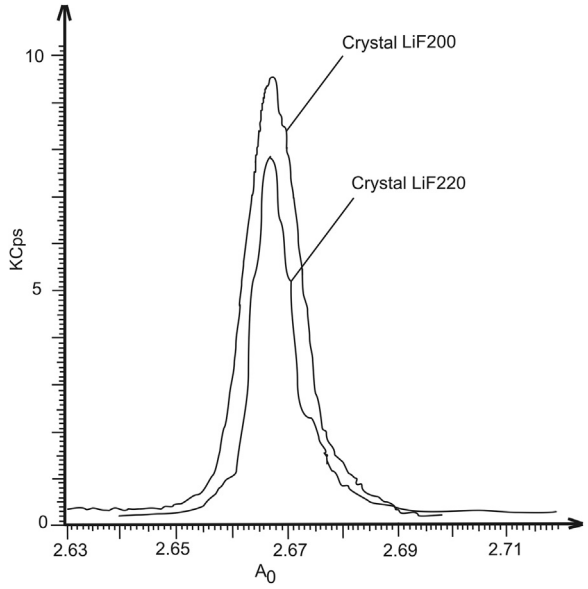

Fig. 3. XRF spectrum of the LaL_{α}-line (measurement time is 300 s).

an X-ray diffractometer DRON-3 (Burevestnik factory, St. Petersburg) equipped with a 3 kW power X-ray tube with a Cu anode. Measurements of the samples were performed at the following conditions: 25 kV operating voltage, 20 mA current, the range of the 2θ angles from 5 to 65 degrees. Identification of the minerals included to the measured samples was performed using the obtained powder diffraction data with the application of the X-ray mineral determinant (Mikheev, 1957).

As it is known, the calcite rich carbonates consist of $CaCO_3$ about 97–99%, on the other hand the concentration of admixtures do not exceed 3%. It is determined that the concentration of the admixtures in the dark-gray marble sample is equal to 2.6% that is linked with the presence of talk, amphibole and chlorite in it. Mineral matter in the white marble sample is presented by talk, siderite, and diopside, which is 0.66% of the total amount. The mineral constituents such as calcite, dolomite, hydromica of muscovite group, and traces of feldspar were observed in the fluorite ore sample (the content of the CaF_2 component is equal to 43.21%).

The determination of rock-forming oxides in the studied samples was carried out by atomic absorption spectrometry (AAS) using a Solaar M6 spectrometer (Thermo Electron, USA) equipped with an automatic sample introduction system for unattended operation. The measurement time of each sample was 100 s. The AAS results indicated that the SiO_2, MnO, MgO, CaO, Na_2O, K_2O, CO_2 concentrations in the light-gray limestone, light- and dark- gray, and white marble samples vary in the ranges (in %): 0.12 – 1.46, 0.03 – 0.04, 0.24 – 0.72, 54.86 – 56.26, 0.02 – 0.05, 0.02 – 0.03, 42.10 – 43.12, respectively. The TiO_2, Al_2O_3, $Fe_2O_{3(total)}$, P_2O_5 concentrations in these samples do not exceed 0.02%, 0.25%, 0.35%, and 0.03%, respectively. Otherwise, the fluorite ore sample has a high concentrations of F (21.05%), SiO_2 (13.69%), Al_2O_3 (0.5%), $Fe_2O_{3(total)}$ (2.02%), MnO (0.49%), MgO (5.10%), K_2O (0.86%), and a lower contents of TiO_2 (< 0.02%), CaO (44.14%), Na_2O (0.027%), and CO_2 (12.30%). In addition, the ranges of rock-forming oxide contents for the carbonatite-like rock samples were (in %) 9.04 – 38.95 for SiO_2, 0.05 – 5.97 for TiO_2, 0.70 – 6.33 for Al_2O_3, 0.28 – 14.94 for $Fe_2O_{3(total)}$, 0.10 – 0.44 for MnO, 1.83 – 21.72 for MgO, 14.30 – 40.81 for CaO, 0.02 – 2.21 for Na_2O, 0.24 – 3.74 for K_2O, 0.03 – 9.08 for P_2O_5, 18.65 – 31.54 for CO_2. The comparison of the above-mentioned values of the rock-forming oxides indicated that the studied carbonate and carbonatite-like rocks belong to different types except the fluorite ore, namely samples with high P concentrations are apatite-enriched, and samples with high Fe and Ti concentrations are magnetite- and rutile-enriched (Savel'eva et al., 2014).

The obtained data about the sample chemical compositions were taken into account when the choice of the ICRMs and HSRMs used for the construction of calibration functions, and the computing the sample surface density provided a “thick” radiating layer.

3.2. Selecting the sample mass to prepare a thick sample

The thickness participating in 99.9% of fluorescent radiation emission was calculated for “infinitely thick” sample according to the expression:

$$dp \geq 4.6/(\mu_{m1}/\sin + \mu_{mi}/\sin \psi), \quad (1)$$

where d is sample thickness (cm); ρ is density of specimen (g cm^{-3}), μ_{m1} and μ_{mi} are total mass attenuation coefficients (cm^2 g^{-1}) at the energy of primary radiation (RhK_{α}-line) and the energy of characteristic X-rays of i-th element, respectively; φ is effective incidence angle ($\varphi = 63^{\circ}$); ψ is take-off angle ($\psi = 45^{\circ}$).

The mass absorption coefficients μ_{m1} and μ_{mi} were computed using the bulk sample composition described in the Section 3.1. A mass of “infinitely thick” sample was evaluated as: $m = d\rho S$, where S is the area exposed to the primary X-rays. Sample holders for the WDXRF spectrometer have a circular aperture of diameter 34 mm; therefore S is equal to 9.1 cm^2. Table 3 contains the mass attenuation coefficients for different analytical lines, values of thickness and masses of “infinitely thick” sample estimated for the calcite-dolomite chloritized marble and metamorphosed carbonatite.

As evident from Table 3, the mass required for the infinite thickness enhances with the increase X-ray energy from 4.95 to 16.52 keV. A maximum mass was calculated for the NbK_{α}-line and equal to 3.07 g, and 1.80 g for the marble and the carbonatite, respectively. The mass attenuation coefficients in the marble sample are less than in the carbonatite sample which contains lower contents of $CaCO_3$ and $MgCO_3$ and a higher content of total Fe_2O_3.

Table 3
The mass attenuation coefficients (μ_{mi}, cm^2 g^{-1}), thickness (d, μm) and mass (m, g) of “infinitely thick” sample.

Line	E, keV	Calcite-dolomite chloritized marble[a]			Metamorphosed carbonatite[b]			SiO_2 matrix[c]			$CaCO_3$ matrix[d]		
		μ_{mi}	d	m	μ_{mi}	d	m	μ_{mi}	d	m	μ_{mi}	d	m
VK_{α}	4.95	195.60	61	0.15	215.60	57	0.13	144.0	84	0.20	272.5	42	0.11
NiK_{α}	7.47	65.25	177	0.43	105.71	113	0.27	43.91	269	0.65	90.80	123	0.31
ZnK_{α}	8.64	43.34	260	0.64	71.37	164	0.39	28.68	402	0.97	60.60	180	0.46
PbL_{β}	12.61	14.72	680	1.67	24.96	416	0.98	9.43	1087	2.61	20.77	466	1.18
SrK_{α}	14.17	10.51	892	2.19	17.92	544	1.28	6.69	1435	3.45	11.85	610	1.55
NbK_{α}	16.62	6.63	1251	3.07	11.27	764	1.80	4.15	2037	4.9	9.29	861	2.19

[a] μ_{m1} = 3.8 cm^2 g^{-1}, ρ = 2.7 g cm^{-3}.
[b] μ_{m1} = 6.5 cm^2 g^{-1}, ρ = 2.6 g cm^{-3}.
[c] μ_{m1} = 2.4 cm^2 g^{-1}, ρ = 2.6 g cm^{-3}.
[d] μ_{m1} = 5.3 cm^2 g^{-1}, ρ = 2.8 g cm^{-3}.

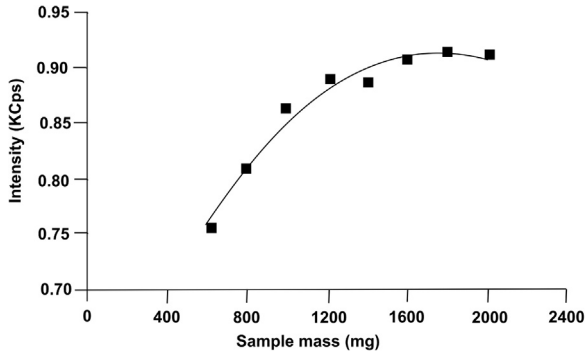

Fig. 4. The experimental dependence of the PbL_{β}-line intensity on the mass of the sample pressed from the powdered HSRM OOKO204.

Additionally, we constructed the experimental dependence of the fluorescence intensity on the sample mass as exemplified by PbL_{β}-line (Fig. 4). The HSRM OOKO204 containing high concentrations of Pb (150 mg kg^{-1}) and Ca (17.83%) was selected to carry out the measurements. As Fig. 4 shows, the XRF intensity grows by 20% with increasing the sample mass from 0.6 to 1.6 g. Further growth in the sample mass up to 2 g insignificantly influences on the PbL_{β}-line intensity that indicates on the achievement of the mass required for the infinite thickness.

The calibration set of the reference materials contains the rocks of the various compositions (see Section 2.3) and its main matrix compounds are $CaCO_3$ and SiO_2. For the SiO_2 matrix the mass attenuation coefficients are about twice as low than for the $CaCO_3$ matrix (Table 3). For instance, for NbK_{α}-line the sample mass required for the infinite thickness is 4.9 g in the SiO_2 matrix, and 2.2 g in the $CaCO_3$ matrix. In order to take into account the matrix variation, next mass was chosen for preparing "thick" sample: 1 g of sample to measure the elements in the energy range 4.47 – 8.64 keV (V, Cr, Co, Ni, Cu, Zn K_{α}-lines; Ba, La, Nd L_{α}-lines; Ce L_{β}-line); and 5 g of a sample to measure the elements in the energy range 12.61 – 16.62 keV (Rb, Sr, Y, Zr, NbK_{α}-lines, PbL_{β}-line).

3.3. X-ray spectra

Optimal background positions for the element analytical lines were chosen. The intensity at the background position must be free from overlaps of spectral element lines presented in the sample, and proximity to the analytical line of the element determined. The relation between the background intensities for each analytical line and the background intensities for the chosen angular positions must not be depend on variations in the chemical composition of the samples studied. This position must be near the element analytical line. So, for the choice of all background positions, the X-ray spectrum of the HSRM OOKO202 (background sediment) was registered in the CaK_{α} – NbK_{α} wavelength range (Fig. 5). For convenience the plot of the XRF spectrum in the VK_{α} – BaK_{α} wavelength range was separated in Fig. 5. The assigned values of the determined element contents in this HSRM are (in mg kg^{-1}): V – 87.0, Cr – 65.0, Co – 13.0, Ni – 31.0, Cu – 44.0, Zn – 54.0, Rb – 85.0, Sr – 250.0, Y – 20.0, Zr – 150.0, Nb – 12.0, Pb – 14.0, Ba – 500.0, La – 30.0, Ce – 50.0, Nd – 20.0 (Govindaraju, 1994). For the estimation of the element concentrations, overlaps of the spectral lines were taken into account using the SPECTRA^{plus} software. As seen from Fig. 5, the TiK_{α} (2θ = 86.12°) line overlaps on the BaL_{α} (2θ = 87.17°) line; TiK_{β} (2θ = 77.25°) – VK_{α} (2θ = 76.92°); VK_{β} (2θ = 69.12°) – CrK_{α} (2θ = 69.34°); FeK_{β} (2θ = 51.72°) – CoK_{α} (2θ = 52.79°); CuK_{β} (2θ = 40.45°) – ZnK_{α} (2θ = 41.81°); RbK_{β} (2θ = 23.75°) – YK_{α} (2θ = 23.79°); SrK_{β} (2θ = 22.42°) – ZrK_{α} (2θ = 22.50°); YK_{β} (2θ = 21.19°) – NbK_{α} (2θ = 21.35°). Thus, the background intensities for the K_{α} -lines of V, Cr, Ni, Zn, Rb, Zr, Nb, the L_{α} -lines of La, Nd, and the CeL_{β} -line has been measured on the short-wave side of their analytical lines. Likewise, the background intensities for the K_{α} -lines of Co, Cu, Sr, Y and the BaL_{α} -line were determined on the long-wave side of their analytical lines.

As an illustration of the chemical composition features of the samples studied, the XRF spectrum of the fluorite ore sample in the CaK_{α} – NbK_{α} wavelength range was also registered (Fig. 6). Note that the feature of the sample chemical composition is a high concentration of CaF_2 combined with a low concentrations of most elements studied. Values of the trace element contents in this sample are (in mg kg^{-1}): V – 8.5, Cr – 5.8, Co – 2.1, Ni – 10.7, Cu – 12.0, Zn – 130.0, Rb – 87.0, Sr – 180.0, Y – 5.0, Zr – 10.0, Nb – 3.1, Pb – 22.0, Ba – 100.0, La – 6.1, Ce – 8.6, Nd – 5.1.

3.4. X-ray spectrum contrast (peak-to-background ratio)

To attenuate the intensity of the X-ray tube radiation and to increase the XRF spectrum contrast, primary radiation filters of a different thickness were applied. The choice of the filter and collimator types was performed using maximum values of the analytical line contrast. Table 4 demonstrates the values of the line contrasts when usage of the different filter thicknesses and collimators as exemplified by the K_{α} -lines of Cr, Co, and Zn. The contrast was assessed by the HSRMs with the high values of the element concentrations such as SDU-1 (4100 mg kg^{-1} of Cr), DVM (1220 mg kg^{-1} of Co), and OOKO201 (390 mg kg^{-1} of Zn). As seen from Table 4, the maximum value of the contrast is occurred at 0.23° collimator and 200 μm Al filter for the CrK_{α} line; for the CoK_{α} line – at 0.17° collimator and 200 μm Al filter; for the ZnK_{α} line – at 0.17° collimator and 500 μm Al filter.

3.5. Quantitative analysis

Calibration curves were constructed using twenty carbonatite, sediment, fluorite and different composition rock the ICRMs and HSRMs. Values of the element concentrations in these reference materials vary within wide ranges (Table 5). The matrix correction method using fixed α-coefficients was carried out by means of the software SPECTRA^{plus} connected to the spectrometer. The corrected concentrations were computed accordingly to the following expression:

$$C_i = m_i I_i \left(1 + \sum_j \alpha'_{ij} I_j\right), \quad (2)$$

where C_i is analyte concentration, I_i is analyte intensity, m_i is slope of the calibration curve, I_j is interfering element intensity, α_{ij} is interelement influence coefficient.

Table 5 presents the calibration data obtained for the rock matrices. The standard deviation (S) characterizing a dispersion point around the calibration line was derived from linear regression equation using least-squares fit to provide minimum value of this one. The comparison indicated that the S values obtained using the fixed α-coefficients were less than the S values achieved without the matrix correction by 1.2 – 14 times (Table 5).

3.6. Analytical figures of merit

The instrumental limit of detection (ILD) and the limit of determination of the WDXRF method (LDM) were computed for each element according to the recommendations from (Rousseau, 2001; Margui et al., 2005). The ILD was defined as being the minimum net intensity of an analyte, which can be detected by an instrument in a given analytical context with a 99.95% confidence level. It was evaluated using the following expression (Margui et al., 2005):

$$\mathrm{ILD} = \frac{4.65}{S_i}\sigma_b, \quad (3)$$

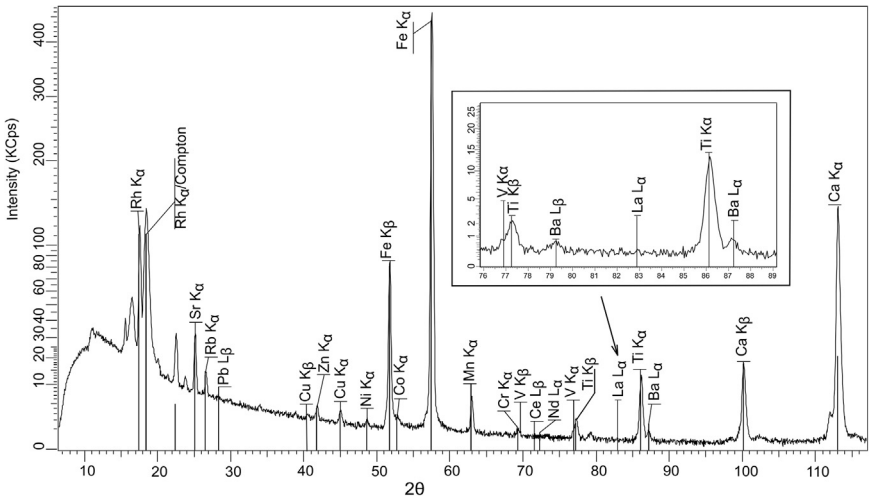

Fig. 5. XRF spectrum of the background sediment HSRM OOKO202 in CaK_α – NbK_α wavelength range. For convenience the plot of the X-ray spectrum in the VK_α – BaK_α wavelength range is separated.

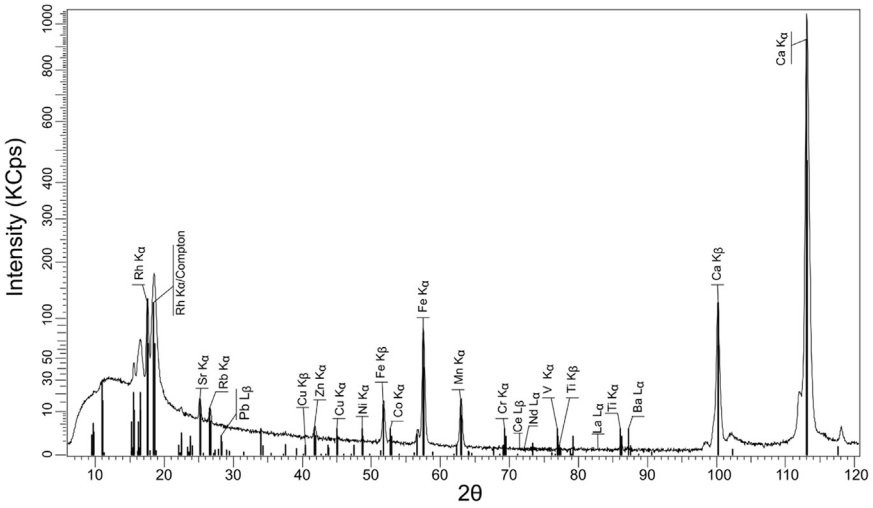

Fig. 6. XRF spectrum of the fluorite ore sample in the CaK_α – NbK_α wavelength range.

Table 4
The contrast of the Cr, Zn and Co K_α-lines when usage different collimators and the primary radiation filters.

K_α- line	Collimator (°)	Peak-to-background ratio (WDXRF spectrum contrast)			
		without filter	Al filter, 12.5 μm	Al filter, 200 μm	Al filter, 500 μm
Cr	0.17	50	57	47	50
	0.23	48	67	70	47
Co	0.17	2.2	1.9	5.5	2.2
	0.23	2.3	2.8	2.6	2.8
Zn	0.17	7.0	6.9	18	21
	0.23	5.4	6.3	12	14

WDXRF spectrum contrast was calculated for the HSRMs with high content of Cr (4100 mg kg^{-1}), Co (120 mg kg^{-1}), Zn (390 mg kg^{-1}).

where S_i is sensitivity (Cps/concentration), σ_b is the standard deviation calculated from several background intensity measurements ($n = 10$).

The results of the ILD calculations for the HSRM OOPE401 "calcareous ooze" are presented in Fig. 7. As it seen, the maximum values of the ILD (1.6 – 4 mg kg^{-1}) were obtained for V, Ba, Ce, Cr, and Nd; for other elements it was ≤ 1 mg kg^{-1}.

The LDM was defined as the smallest concentration of an analyte that can be reliably quantified by a given analytical method with a 95.4% confidence level (Rousseau, 2001; Margui et al., 2005). It was calculated from a series of ten replicate specimens ($n = 10$) prepared from the representative sample of the carbonatite-like rock:

$$\mathrm{LDM} = 2\sqrt{\frac{\sum_{m=1}^{n}(C_m - \overline{C})^2}{n-1}}; \quad \overline{C} = \frac{\sum_{m=1}^{n} C_m}{n}. \tag{4}$$

The concentration of each element and the obtained LDM values are shown in Table 6. It can be seen, the LDM values do not exceed 5 mg kg^{-1} for most of the elements determined.

In order to test repeatability of the WDXRF method, 10 tablets were prepared from the single representative sample of the carbonatite-like rock and measured once, than one of the tablets was measured 10 times (Rousseau, 2001; Margui et al., 2005). The average value of the analytical line intensity and the relative standard deviations (RSD) of the measurement results are given in Table 7. As it can be seen from the Table 7, the uncertainty due to the sample preparation is higher than the uncertainty due to the measurements in most cases, but for both experiments the RSD values are acceptable and do not exceed 5%.

Additionally, the reproducibility of the measurements was evaluated (Margui et al., 2005). The tablet used for the repeatability study was measured tree times during a period of 1 month (Table 7). The obtained RSD values were lower than 5% that indicating high stability of the measurements (Table 8).

The accuracy of the proposed XRF method was checked by

Table 5
Calibration data obtained for the rock matrices.

Element	Number of the ICRMs and HSRMs	Calibration range (mg kg^{-1})	Line overlap correction	Influence coefficients (α-correction)	S[a] (mg kg^{-1})	
					I[b]	II[c]
V	20	6 – 960	TiK_α	SiK_α, CrK_α, MnK_α	22	15
Cr	25	4.3 – 2000	VK_α, MnK_α	CaK_α, TiK_α, FeK_α	27	5
Co	20	2 – 106	FeK_α	SiK_α,VK_α, MnK_α	5	3
Ni	20	4.4 – 2240	RbK_α	SiK_α, CaK_α, FeK_α	22	14
Cu	25	8 – 240	NiK_α	CaK_α, FeK_α	9	7
Zn	20	10 – 610	CuK_α	CaK_α	21	9
Pb	20	3 – 280	–	CaK_α, FeK_α	3	2
Rb	23	5 – 450	SrK_α	ZrK_α, YK_α	8	4
Sr	20	5 – 4600	–	CaK_α	340	25
Y	25	4 – 959	RbKα, SrK_α	SiK_α, ZrK_α	9	7
Zr	22	10 – 2200	SrK_α	CaK_α, YK_α	18	13
Nb	20	5 – 380	ZrK_α	FeK_α, SrK_α, YK_α	24	2
Ba	25	8.8 – 6900	LaL_α, TiK_α	SiK_α, CaK_α, MnK_α	207	115
La	22	1.4 – 400	CeL_β	CaK_α, MnK_α, TiK_α, BaL_α	22	4
Ce	20	3.4 – 1000	AsK_α, PbL_β, NdL_α	SiK_α, TiK_α, FeK_α, BaL_α	16	14
Nd	23	2.7 – 1200	CeL_β, LaL_α, BaL_α	CaK_α, TiK_α, FeK_α	32	7

[a] Standard deviation.
[b] Without correction of the matrix effects.
[c] With accounting of the matrix effects (α-correction).

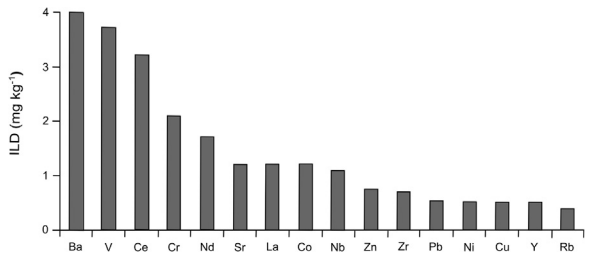

Fig. 7. Instrumental detection limits calculated for the calcareous ooze HSRM OOPE401.

Table 6
Limits of the determination (mg kg^{-1}) of the WDXRF method evaluated in a carbonatite-like rock specimen, $n = 10$.

Element	Concentration (mg kg^{-1})	LDM[a]
V	420	5.5
Cr	373	4.4
Co	43	2.9
Ni	225	8.0
Cu	41	1.3
Zn	332	2.5
Pb	55	3.5
Rb	45	1.8
Sr	1213	11.9
Y	58	2.3
Zr	619	8.1
Nb	146	4.8
Ba	875	15.8
La	102	6.6
Ce	198	7.0
Nd	127	4.2

[a] The limit of determination of the WDXRFS.

measuring the HSRM GPOS302 (dolo limestone) and the reference sample CH-1 (marine sediment). The data for CH-1 were obtained by the international proficiency testing programme for analytical geochemistry laboratories, report on round 10, GeoPT10 (Potts et al., 2001). Comparison of the achieved results (Table 9) showed that the data obtained by the proposed WDXRF technique provide a good agreement with the reference values. Recovery values were found to be satisfactory and ranged between 85% and 115%.

In order additionally to validate the accuracy, the concentrations

Table 7
Comparison of the WDXRF results of 1 measurement on 10 different tablet rock specimens and of 10 measurements on the same tablet.

Analyte	10 tablets / 1 measurement		1 tablet / 10 measurements	
	Intensity (KCps)	RSD (%)	Intensity (KCps)	RSD (%)
V	0.402	0.7	0.399	0.5
Cr	0.537	0.8	0.543	0.5
Co	0.102	4.8	0.099	3.3
Ni	3.226	1.9	3.218	2.1
Cu	0.270	2.0	0.269	1.3
Zn	1.165	0.2	1.170	0.4
Pb	0.505	0.9	0.496	0.5
Rb	0.646	1.9	0.644	1.5
Sr	18.631	0.6	18.721	0.3
Y	1.302	2.3	1.269	1.7
Zr	13.437	0.5	13.443	0.6
Nb	2.945	1.7	3.029	0.8
Ba	0.930	1.6	0.921	0.9
La	0.074	1.6	0.079	2.0
Ce	0.071	1.9	0.073	2.1
Nd	0.082	2.2	0.079	2.8

Table 8
Study of the reproducibility of the measurements during a period of 1 month.

Analyte	Intensity (KCps)			RSD[a] (%)
	1 day	1 week	1 month	
V	0.401	0.394	0.399	1.0
Cr	0.540	0.539	0.539	0.5
Co	0.101	0.095	0.097	4.5
Ni	3.201	3.217	3.216	1.7
Cu	0.263	0.263	0.270	1.4
Zn	1.164	1.163	1.156	0.3
Pb	0.491	0.502	0.496	1.0
Rb	0.640	0.640	0.651	1.3
Sr	18.627	18.508	18.687	0.5
Y	1.315	1.304	1.326	1.0
Zr	13.329	13.470	13.473	0.8
Nb	2.950	2.971	2.980	0.8
Ba	0.912	0.921	0.920	1.2
La	0.077	0.080	0.074	1.9
Ce	0.074	0.075	0.072	2.5
Nd	0.081	0.080	0.081	2.1

[a] Relative standard deviation.

Table 9
Concentration (mg kg^{-1}) (mean ± standard deviation, $n = 3$) obtained for the dolo limestone HSRM GPOS302 and marine sediment CH-1 by the proposed WDXRF method.

Element	GPOS302		CH-1	
	C_{WDXRF}	C_{cert} [a]	C_{WDXRF}	C_{GeoPT} [b]
V	24 ± 2	23 ± 6	86 ± 4	87.6 ± 1.4
Cr	10 ± 0.4	9 ± 3	60 ± 1	60.6 ± 1.3
Co	2.6 ± 0.4	2.3 ± 0.3	12 ± 1	12.49 ± 0.27
Ni	5.3 ± 0.4	5 ± 2	43 ± 2	43.8 ± 0.70
Cu	4.6 ± 0.5	4 ± 2	24 ± 0.9	23.05 ± 0.59
Zn	29 ± 0.6	30 ± 10	96 ± 3	94.2 ± 1.1
Pb	12 ± 0.7	13 ± 3	20 ± 1.2	20.15 ± 0.39
Rb	15 ± 0.2	15 ± 2	109 ± 0.5	107.3 ± 0.9
Sr	445 ± 15	440 ± 80	501 ± 10	502.8 ± 4.0
Y	10 ± 0.4	Not certified	23 ± 0.7	22.92 ± 0.39
Zr	28 ± 1.2	27 ± 6	132 ± 0.4	133.7 ± 2.0
Nb	8 ± 0.3	7 ± 3	12 ± 1.1	12.80 ± 0.27
Ba	55 ± 3	50 ± 20	497 ± 10	493.5 ± 4.7
La	9 ± 2	8 ± 2	31 ± 1.2	31.10 ± 0.41
Ce	14 ± 2.5	16 ± 4	60 ± 1	60.5 ± 0.7
Nd	8.9 ± 2	Not certified	29 ± 3	26.24 ± 0.32

[a] Certified value.
[b] Accepted value in the GeoPT programme, report on round 10.

determined via WDXRF were compared to those obtained by inductively coupled plasma mass spectrometry (ICP-MS). The sample preparation for analysis by the ICP-MS method was performed using open acid digestion technique described in (Panteeva et al., 2003). Table 10 exemplifies the WDXRF and ICP-MS results obtained for the fluorite ore, dark gray marble, and carbonatite-like rock samples. It can be seen that the relative disagreements between the WDXRF and ICP-Ms results are not more than 10%.

4. Conclusion

A technique for the multielemental analysis of the sedimentary rocks with high calcium content has been developed using the WDXRF spectrometer. Analytical strategies were generated for the determination of some trace elements (V, Cr, Co, Ni, Cu, Zn, Pb, Ba, La, Ce, Nd, Rb, Sr, Y, Zr, and Nb) selected for the study of the genesis and the accumulation of the sedimentary rocks collected from the central part of the Republic of Buryatia and the western shore of the lake Baikal (Russia). The sample preparation procedure was chosen taking into account the infinite thickness calculations. The studied samples were pressed as tablets using 1 g of sample powder for the determination of V, Cr, Co, Ni, Cu, Zn, Ba, La, Nd, Ce and 5 g for the determination of Rb, Sr, Y, Zr, Nb, Pb. Optimal instrumental measuring conditions were chosen for each element to achieve high peak-to-background ratio and overlaps of the spectral lines were taken into account. Combination of the sediment and the rock reference materials to construct the calibration curves provided wide calibration range of the concentrations. The matrix correction method based on the usage of α-coefficients was employed to decrease a value of the standard deviation characterizing a dispersion point around the calibration line by 1.2–14 times depending on the element determined. The instrumental limit of the detection, the limit of the determination, the repeatability, the reproducibility and the accuracy of the WDXRF method were found to be satisfactory and illustrate the viability of the technique. The proposed WDXRF technique can be applied for the environmental and geological studies of different natural objects.

Table 10
Comparison of the WDXRF and ICP-MS results (mg kg^{-1}) (mean ± standard deviation, $n = 3$).

Element	Method	Fluorite ore, $C \pm \Delta$ [a]	Dark gray marble, $C \pm \Delta$	Carbonatite-like rocks, $C \pm \Delta$		
				1	2	3
V	WDXRF	8.5 ± 0.7	11 ± 1	432 ± 15	110 ± 5	258 ± 7
	ICP-MS	9.7 ± 1.0	9.3 ± 1	435 ± 20	114 ± 6	261 ± 13
Cr	WDXRF	5.8 ± 0.6	7.3 ± 0.7	363 ± 10	57 ± 1.5	130 ± 4
	ICP-MS	7 ± 0.6	7.6 ± 0.8	371 ± 20	56 ± 2	128 ± 6
Co	WDXRF	< 2	< 2	44 ± 4	11 ± 2	16 ± 1
	ICP-MS	2.1 ± 0.1	1.5 ± 0.1	46 ± 2	13 ± 0.6	16.5 ± 0.8
Ni	WDXRF	10.7 ± 0.8	8.9 ± 0.7	225 ± 8	56 ± 3	55 ± 2
	ICP-MS	13.1 ± 1.3	10.1 ± 1	230 ± 10	58 ± 3	56 ± 3
Cu	WDXRF	12 ± 1.0	5.1 ± 0.7	41 ± 5	5.8 ± 0.8	9.8 ± 0.8
	ICP-MS	11.7 ± 0.6	4.5 ± 0.2	37 ± 2	5.2 ± 0.3	10.3 ± 0.5
Zn	WDXRF	130 ± 4.2	16 ± 1	330 ± 11	65 ± 2	90 ± 5
	ICP-MS	139 ± 11	18 ± 1	320 ± 16	63 ± 3	93 ± 5
Pb	WDXRF	22.0 ± 1.0	3.7 ± 0.3	119 ± 4	40 ± 5	37 ± 2
	ICP-MS	24.0 ± 1.9	3.1 ± 0.3	121 ± 6	43 ± 2	38 ± 2
Rb	WDXRF	87 ± 2	< 1	54 ± 3	17 ± 1.2	20 ± 1
	ICP-MS	89 ± 3	0.9 ± 0.05	55 ± 3	15 ± 0.8	19.8 ± 1
Sr	WDXRF	180 ± 7	256 ± 7	940 ± 12	995 ± 15	1600 ± 15
	ICP-MS	167 ± 8	260 ± 13	929 ± 30	982 ± 20	1589 ± 20
Y	WDXRF	4.5 ± 0.5	< 1	32 ± 3	420 ± 8	270 ± 7
	ICP-MS	5.3 ± 0.3	0.8 ± 0.04	30 ± 2	414 ± 10	265 ± 13
Zr	WDXRF	10 ± 2	< 2	152 ± 7	42 ± 3	41 ± 2
	ICP-MS	12 ± 0.6	1.7 ± 0.1	147 ± 7	44 ± 2	42 ± 2
Nb	WDXRF	< 1	< 1	330 ± 10	135 ± 6	230 ± 5
	ICP-MS	0.9 ± 0.05	0.1 ± 0.01	338 ± 17	142 ± 7	222 ± 11
Ba	WDXRF	100 ± 8	85 ± 5	870 ± 15	910 ± 10	755 ± 10
	ICP-MS	110 ± 5	80 ± 4	895 ± 20	901 ± 20	770 ± 15
La	WDXRF	5.5 ± 0.9	< 1.2	102 ± 6	450 ± 8	370 ± 5
	ICP-MS	4.6 ± 0.3	0.5 ± 0.03	98 ± 5	453 ± 10	372 ± 12
Ce	WDXRF	8.0 ± 0.8	< 3	190 ± 8	980 ± 12	752 ± 7
	ICP-MS	9.2 ± 0.5	1.1 ± 0.1	200 ± 10	987 ± 10	760 ± 10
Nd	WDXRF	5.0 ± 0.6	< 2	128 ± 9	690 ± 8	353 ± 4
	ICP-MS	4.5 ± 0.2	0.7 ± 0.04	120 ± 6	688 ± 15	356 ± 18

[a] Confidence intervals were computed at the confidence level $P = 0.95$ and the number of the measurements $n = 6$.

Acknowledgments

The authors gratefully acknowledge analysts Z.F. Ushchapovskaia, N.N. Ukhova, T.V. Popova, E.G. Koltunova for the analysis of the carbonate samples by the X-ray diffraction and atomic absorption spectrometry. We appreciate to Ph.D. V.B. Savel'eva for the presented collection of the carbonatite-like rock samples.

The research was financially supported by the Federal Agency of Scientific Organization (FASO Russia) program (№ 0346–2014-0001). This study was performed using equipment located at the Center for Geodynamics and Geochronology (Institute of the Earth's Crust, SB RAS, Irkutsk).

References

Applied Physics Institute at Irkutsk State University (API ISU), 1970. 〈http://www.api.isu.ru/about_us.htm〉 (Accessed 8 June 2016).

Arnautov, N.V., 1990. Reference Materials of the Chemical Composition of Natural Materials. Nauka Press, Novosibirsk (in Russian).

Arriolabengoa, M., Iriarteb, E., Aranburua, A., Yustaa, I., Arrizabalagad, A., 2015. Provenance study of endokarst fine sediments through mineralogical and geochemical data (Lezetxiki II cave, northern Iberia). Quatern. Int. 364, 231–243. http://dx.doi.org/10.1016/j.quaint.2014.09.072.

Babatunde, A., Ademola, B.W., 2014. Discontinuities effect on drilling condition and performance of selected rocks in Nigeria. Int. J. Min. Sci. Tech. 24, 603–608. http://dx.doi.org/10.1016/j.ijmst.2014.07.008.

Bronnitskaya geological-geochemical expedition, 1970. 〈http://bggevin.okis.ru/〉 (Accessed 9 June 2016).

Catalog of Reference Materials: Institute of Geochemistry, 2013. SB RAS. 〈http://igc.irk.ru/ru/uslugi/eksperimentalnye-obraztsy〉 (Accessed 8 June 2016).

Govindaraju, K., 1994. Compilation of working values and sample description for 383 geostandards. Geostand. Geoanal. Res. 18, 1–158.

James, N.P., Jones, B., 2015. Origin of Carbonate Sedimentary Rocks. Wiley, American Geophysical Union.

Jones, M.H., Wilson, B.W., 1991. Rapid method for the determination of the major components of magnesite, dolomite and related materials by X-ray Spectrometry. Analyst 116, 449–452. http://dx.doi.org/10.1039/AN9911600449.

Letnikova, E.F., 2005. Geochemical types of carbonate deposits within different geodynamic settings of north-eastern part of Paleoasian Ocean. Lithosphere 1, 70–81 (in Russian).

Margui, E., Hidalgo, M., Queralt, I., 2005. Multielemental fast analysis of vegetation samples by wavelength dispersive X-ray fluorescence spectrometry: possibilities and drawbacks. Spectrochim. Acta 60 B, 1363–1372. http://dx.doi.org/10.1016/j.sab.2005.08.004.

Markov, V., 2011. Geo-ecological Investigation of Sediments of Inland Basins of the Valaam Archipelago. 138. Proceedings of Russian State Pedagogical University, pp. 95–100.

Mikheev, V.I., 1957. X-ray Mineral Determinant, first ed. Gosgeoltech Press, Moscow.

Mineral resources of the Republic of Buryatia, 2015. 〈http://www.baikal-center.ru/books/element.php?ID=1163〉 (Accessed 31 May 2016).

OST 41-08-212-04, 2004. Industrial Standard. Quality Control of Analytical Works. Russia Scientific Research Institute of Mineral Resources. Standardinform Press, Moscow (in Russian).

Panteeva, S.V., Gladkochoub, D.P., Donskaya, T.V., Markova, V.V., Sandimirova, G.P., 2003. Determination of 24 trace elements in felsic rocks by inductively coupled plasma mass spectrometry after lithium metaborate fusion. Spectrochim. Acta 58 B 341–350. http://dx.doi.org/10.1016/S0584-8547(02)00151-9.

Potts, P.J., Thompson, M., Webb, P.C., Watson, J.S., Yimin, W., 2001. GeoPT10 – an international proficiency test for analytical geochemistry laboratories – report on round 10 / December 2001 (ch-1 marine sediment). 〈http://www.geoanalyst.org/geopt/GeoPT10Report.pdf〉 (Accessed 14 July 2016).

Revenko, A.G., 2002. X-ray fluorescence analysis of rocks, soils and sediments. X-ray Spectrom. 31, 264–273. http://dx.doi.org/10.1002/xrs.564.

Rousseau, R.M., 2001. Detection limit and estimate of uncertainty of analytical XRF results. Rigaku J. 18, 33–47.

Santos, I.R., Favaro, D.I.T., Schaefer, C.E.G.R., Silva-Filho, E.V., 2007. Sediment geochemistry in coastal maritime Antarctica (Admiralty Bay, King George Island): evidence from rare earth and other elements. Mar. Chem. 107, 464–474. http://dx.doi.org/10.1016/j.marchem.2007.09.006.

Sarbajna, C., Durani, S., Nayak, S., Krishnakumar, M., Karuppan, V.M., Shivkumar, K., 2013. Determination of U, S, V, Cu, Zn, Sr, Mo, and Ce in carbonate rocks by wavelength dispersive X-ray fluorescence spectrometry and inductively coupled plasma optical emission spectrometry. At. Spectrosc. 34, 31–38.

Savel'eva, V.B., Bazarova, E.P., Danilov, B.S., 2014. New finds of carbonatite-like rocks in the Western Baikal Region. Dokl. Earth Sci. 459, 1483–1487. http://dx.doi.org/10.1134/S1028334×14120113.

Schlotz, R., 2006. Introduction to X-ray Fluorescence Analysis. Schoolbook. Bruker AXS, Moscow, Russia.

Service Manual, 2007. S8 TIGER XRF Spectrometer. Bruker AXS, Berlin.

Sklyarov, E.V., Gladkochub, D.P., Donskaya, T.V., Ivanov, A.V., Letnikova, E.F., Mironov, A.G., Barash, I.G., Bulanov, V.A., Sizykh, A.I., 2001. Interpretation of Geochemical Data. Intermet Inzhiniring, Moscow (in Russian).

Sliwinski, M.G., Spaleta, K.J., Meyer, F.J., Hutton, E.M., Newberry, R.J., Trainor, T.P., Severin, K.P., Whalen, M.T., 2012. Making low concentration in-house pressed pellet trace element standards for carbonate rock analyses by WD-XRF. Chem. Geol. 298–299, 97–115. http://dx.doi.org/10.1016/j.chemgeo.2011.12.027.

SPECTRA^{plus}, 2010. Software P ackage for X-Ray Spectrometers. Version 2.2.3.1. Bruker AXS Karlsruhe, Germany.

Wheeler, B.D., 1999. Analysis of limestones and dolomites by X-ray fluorescence. Rigaku J. 16, 16–25.

Zaigraevskii area, 2015. 〈https://ru.wikipedia.org/wiki/〉 (Accessed 31 May 2016).

Zwolinski, Z., Rachlewicz, G., Mazurek, M., Paluszkiewicz, R., 2007. The geoecological model for small tundra lakes, Spitsbergen. Landf. Anal. 5, 113–118.